

# Radio jet interactions in the radio galaxy PKS 2152-699

R.A.E. Fosbury<sup>1\*</sup>, R. Morganti<sup>2,3</sup>, W. Wilson<sup>2</sup>, R.D. Ekers<sup>2</sup>,  
S. di Serego Alighieri<sup>4</sup>, C.N. Tadhunter<sup>5</sup>

<sup>1</sup> *Space Telescope-European Coordinating Facility, D-85748 Garching bei München, Germany*

<sup>2</sup> *CSIRO, Australia Telescope National Facility, PO Box 76, Epping, NSW 2121, Australia*

<sup>3</sup> *Istituto di Radioastronomia, CNR, via Gobetti 101, 40129 Bologna, Italy*

<sup>4</sup> *Osservatorio Astrofisico di Arcetri, largo E.Fermi 5, I-50125, Firenze, Italy*

<sup>5</sup> *Department of Physics, University of Sheffield, Sheffield S3 7RH, England*

Accepted , Received

## ABSTRACT

We present radio observations of the radio galaxy PKS 2152-699 obtained with the Australia Telescope Compact Array (ATCA). The much higher resolution and s/n of the new radio maps reveals the presence of a bright radio component about 10 arcsec NE of the nucleus. This lies close to the highly ionized cloud previously studied in the optical and here shown in a broadband red snapshot image with the HST PC 2. It suggests that PKS 2152-699 may be a jet/cloud interaction similar to 3C277.3. This could cause the change in the position angle (of  $\sim 20^\circ$ ) of the radio emission from the inner to the outer regions. On the large scale, the source has Fanaroff & Riley type II morphology although the presence of the two hot-spots in the centres of the lobes is unusual. The northern lobe shows a particularly relaxed structure while the southern one has an edge-brightened, arc-like structure.

**Key words:** galaxies: active – galaxies: interactions – galaxies: radio continuum

## 1 INTRODUCTION

Extended-emission line regions (EELR) are a common feature of powerful radio galaxies. In the high-redshift objects, these regions display a particular range of phenomena which are of especial interest for studies of the properties of AGN and the formation and evolution of their host galaxies. Extended line and rest-frame ultraviolet continuum emission appears, above redshifts of around 0.8, to be aligned with the extended double radio structures (McCarthy et al. 1987, Chambers, Miley & van Breugel 1987) although the radio and optical emitting regions are not necessarily co-extensive. In some cases, however, there is a close correlation between the radio emission and the EELR over distances of tens of kiloparsecs and extreme kinematic components are observed associated with the radio emission (e.g., McCarthy et al. 1987, McCarthy 1993), suggesting a continuing interaction between the radio plasma and the ISM.

In an effort to understand the high redshift phenomena in more detail, we are studying selected low redshift objects which exhibit some of these characteristics. The correlation between EELR and radio emission is not so common at low  $z$ . Nevertheless, a number of cases of regions of ionized gas

found coincident or close to a radio feature — either jet or lobe — are known and, in some cases, well studied (e.g., NGC 7385, Simkin & Ekers 1979; 3C171, Heckman, van Breugel & Miley 1984; 3C277.3, van Breugel et al. 1985a; Minkowski’s object, van Breugel et al. 1985b; 4C 29.30, van Breugel et al. 1986; Centaurus A, Morganti et al. 1990; 3C285, van Breugel & Dey 1993; PKS 2250-41, Clark et al. 1997 and PKS 1932-43, Villar-Martin et al. in prep.). Some of them are believed to represent an interaction between the radio plasma and the ISM: a ‘jet/cloud’ interaction.

PKS 2152-699 is a powerful, nearby radio galaxy ( $z = 0.0282$ , 1 arcsec = 0.8 kpc for  $H_0 = 50 \text{ km s}^{-1} \text{ Mpc}^{-1}$ ) with a cloud of highly ionized gas observed at about 10 arcsec ( $\sim 8$  kpc) from the nucleus. The very highly ionized cloud (HIC), with ions up to  $\text{Fe}^{9+}$  and a blue optical continuum, was first studied in detail by Tadhunter et al. (1987, 1988). Although the HIC has a velocity very similar to systemic, broad, blue wings in the [O III] emission lines (up to 3000 km/s from the systemic velocity of the HIC and galaxy) have been observed. The presence of some gas at high velocities led Tadhunter et al. (1988) to conclude that the cloud could possibly be related to interaction between the radio plasma and the ISM.

However, later work (di Serego Alighieri et al. 1988; Fosbury et al. 1990) showed that the HIC has a very blue

\* Email: rfosbury@eso.org

optical to near-UV continuum with 10% linear optical polarization and the E-vector perpendicular to the position angle of the nucleus-HIC axis. The existence of the blue, polarized continuum led di Serego Alighieri et al. (1988) to suggest that this resulted from the scattering by dust in the cloud of beamed radiation from the nucleus. In this picture, the source of ionization for the cloud is UV radiation from the nucleus. The presence of transverse ionization gradients also lent support to the beamed illumination model (Tadhunter et al. 1988).

The quality of the radio maps available until now (Christiansen et al. 1977, Tadhunter et al. 1988, Jones & McAdam 1992, Fosbury et al. 1990) does not allow a detailed investigation of the radio emission in the region of the HIC. To search for clear evidence of a jet/cloud interaction in PKS 2152-699, we have made new radio observations with the Australia Telescope Compact Array (ATCA) at both 3 and 6 cm wavelength. In presenting the radio data and comparing with the optical morphology, we use a broadband red image of the galaxy taken with the HST PC 2 available from the public archive. VLBI observations of the nuclear region were presented by Tingay et al. (1996).

Subsequent papers will report a series of infrared, optical, ultraviolet and X-ray observations which allow us to study the broad-band spectral energy distribution of the nucleus and separate components within the interaction site.

## 2 OBSERVATIONS

The observations reported in this paper were made on the 19 and 23 January, 21 March and 1 April 1992 using the four 6-km configurations available with ATCA and the standard continuum correlator setup with a bandwidth of 128 MHz and 32 channels. The two simultaneous frequencies were set to 4.74 and 8.64 GHz. The source was observed for 12h in each configuration. The data were calibrated by using the MIRIAD package (Sault, Teuben & Wright 1995), which is necessary for the calibration of the polarization of ATCA data. The flux scale is based on the recent compilation of measurements of the primary calibrator PKS 1934-638 by Reynolds (1996) which corresponds to 5.91 Jy at 4.7 GHz and 2.84 at 8.6 GHz. This differs from the previous calibration in use at the Compact Array by (new-old) -8.1% at 4.7 GHz and +9.8% at 8.6 GHz.

At 4.7 GHz we have made images with both uniform weight and using the “robust” parameter equal to 0.5. The former gives the full resolution of  $1.39 \times 1.44$  (PA =  $11.7^\circ$ ) while the latter gives a beam of  $2.3 \times 2.1$  arcsec (PA =  $58^\circ$ ). Using the “robust” parameter we were able to give more weight to the short baselines and therefore the extended low-brightness emission is better imaged. The total intensity map at 4.7 GHz at lower resolution is shown in Fig. 1. At 8.6 GHz, the data have a full resolution of  $0.8 \times 0.9$  arcsec (PA =  $-26^\circ$ ). The rms noise of the total intensity maps is about  $0.80 \text{ mJy beam}^{-1}$  in the 4.7 GHz map and  $0.65 \text{ mJy beam}^{-1}$  in the 8.6 GHz map.

The total fluxes derived from these synthesis observations are given in Table 1. At 8.6 GHz, it appears to be lower than single dish observations ( $6.22 \text{ Jy}$  at 8.4 GHz from Wright & Otrupcek 1990), most likely due to missing short spacings.

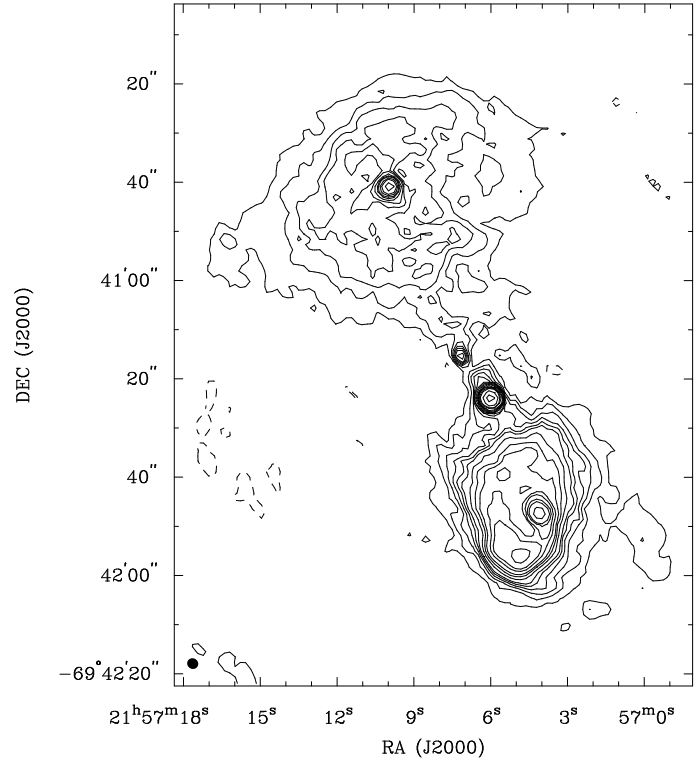


**Figure 1.** ATCA 4.8 GHz image of PKS 2152-699. The contour levels are  $-1, 1, 2, 3, 4, 5, 6, 8, 10, 12, 16, 20, 30, 40, 80, 160 \times 3 \text{ mJy beam}^{-1}$ .

**Table 1.** Radio Properties of PKS 2152-699

Region	$I_{4.7\text{GHz}}^a$ Jy	$m_{4.7\text{GHz}}^a$ %	$I_{8.6\text{GHz}}^b$ Jy	$\alpha_{8.6}^{4.7}$
Total	9.94	24.0	3.80	–
Core	0.77	2.0	0.81	+0.10
HIC	0.04	21.9	0.017	-1.10
N lobe	3.61	26.4	–	–
N hot spot	0.21	14.6	0.09	-0.87
S lobe	5.41	21.2	2.30	–
S hot spot	0.56	13.8	0.25	-0.92

a) beam size  $2.1 \times 2.3$  arcsec

b) beam size  $1.5 \times 1.6$  arcsec

We have also obtained the images of the Stokes parameters ( $Q, U$ ), the polarized intensity image ( $P = (Q^2 + U^2)^{1/2}$ ) and position-angle image ( $\chi = 0.5 \arctan(U/Q)$ ). Here we present these images only for the data at 4.7 GHz because at 8.6 GHz the polarization maps are not completely reliable, probably due to instrumental polarization affecting the data in the earliest days of ATCA when the data presented here were collected. The rms noise of the  $Q$  and  $U$  maps at 4.7 GHz is about  $0.17 \text{ mJy beam}^{-1}$ .

The polarized intensity and the fractional polarization ( $m = P/I$ ) were estimated only for the pixels for which  $P > 5\sigma_{QU}$ . Fig. 2 shows a greyscale image of the polarized intensity while Fig. 3 shows contours of the total intensity with superimposed vectors whose length is proportional to the fractional polarization and whose position angle is that

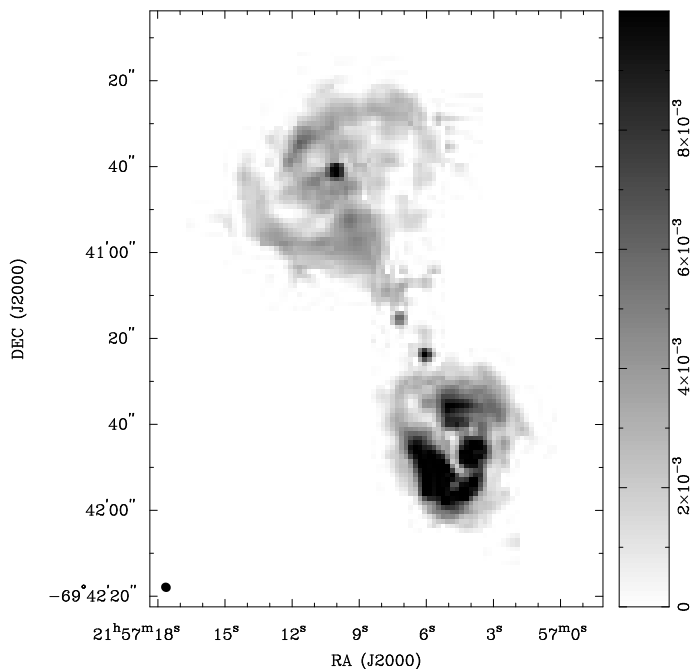


**Figure 2.** Greyscale image of the polarized intensity of PKS2152-69 at 6cm. The range is between 0 and 10 mJy.

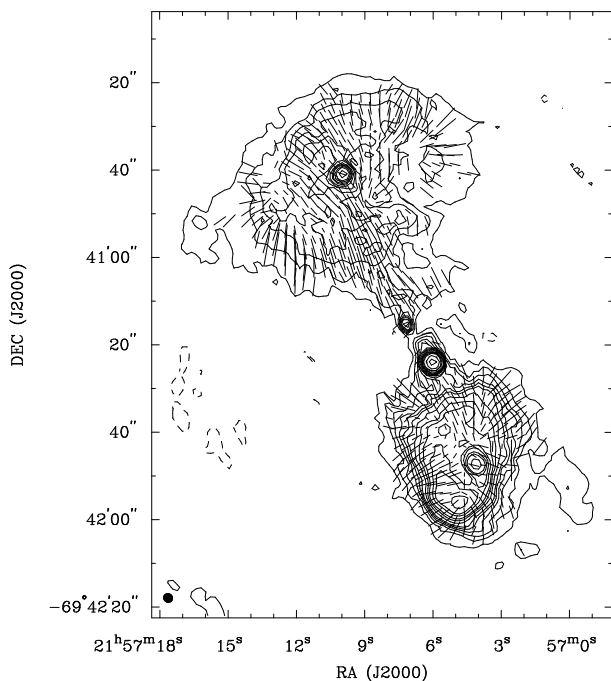


**Figure 3.** Contours (as in Fig. 1) of the total intensity at 4.8 GHz image of PKS 2152-699 with superimposed vectors whose length is proportional to the fractional polarization and whose position angle is that of the electric field.

of the electric field. The mean fractional polarization of the different regions is given in Table 1.

In order to estimate the spectral index in some regions we have produced an 8.6 GHz map degrading the resolution to match that of the 4.7 GHz (uniform weight). The spectral index  $\alpha_{8.6}^{4.7}$  (defined as  $S \propto \nu^\alpha$ ) was estimated only from the regions with signal above  $5\sigma_I$  in both maps. The values of the spectral index must be interpreted with caution because

the observations were not made with matched arrays: a more complete study of both polarization and spectral index is in progress and will be presented in a forthcoming paper.

## 2.1 Results

Compared to the previous observations from the Molonglo Synthesis Telescope (Tadhunter et al. 1988) and from ATCA (Fosbury et al. 1990), the radio structure is now shown more clearly. An important feature is the bright source  $\sim 10$  arcsec NE of the nucleus, i.e., at the same distance and similar—but not identical—position angle from the nucleus as the HIC. This component, which we call RC, was not visible in the previous low resolution radio images available for PKS 2152-699 although it was seen with a lower significance in the early ATCA image by Fosbury et al. (1990).

The new radio images show that PKS 2152-699, although strictly classified as a Fanaroff & Riley type II source on the basis of the ratio of hot-spot separation to total source length, it is unusual in showing the hot-spots near the centres of the lobes. This behaviour, which is intermediate between FR I and II types, has been observed before (e.g. Capetti, Fanti & Parma 1995) in objects with radio power on the border between the two classes ( $\log P \sim 25.5$   $\text{W Hz}^{-1}$  at 4.7 GHz). The total radio power of PKS 2152-699 ( $\log P = 25.61$   $\text{W Hz}^{-1}$  at 4.7 GHz) is indeed typical of the transition region between FR I and II galaxies. For the objects studied by Capetti et al. (1995), the peculiar morphology could be due to precession of the central engine or perhaps by an externally-induced change in jet direction. The southern lobe of PKS 2152-699 shows an edge-brightened, arc-like structure which suggests jet precession. The bright spot then represents the primary hot-spot and the current point of impact of the jet with the ISM while the arc-like bright emission represents the previous impact points during the change of direction of the jet (see also the simulations in Cox, Gull & Scheuer 1991). Something similar could also occur in the northern lobe with the radio plasma far away from the hot-spot could represent the backflow from previous, more distant, fading hot spots. A similar scenario, with the lobe considered as a relic from earlier jet activity, has been suggested for 3C111 (Linfield & Perley 1984). Hot-spots in the middle of the lobe can also be due to projection effects or the result of an interaction moving the jet direction. The spectral indices observed in the hot-spots are unusually steep ( $\alpha_{8.6}^{4.7} \sim -0.9$ ) which could be due to the result of a spectral break between these two frequencies. This has been observed in the knots of 3C277.3, an object with many characteristics in common with PKS 2152-69.

The radio emission in PKS 2152-699 is asymmetric both in flux and core/lobe distance. The southern lobe extends for approximately 30 arcsec (24 kpc) while the northern extends to 45 arcsec (36 kpc). We do not find clear evidence for a jet, but a thin, low brightness emission bridge between the nucleus and the northern lobe is visible at 4.7 GHz. Although very weak, the total emission from the northern lobe shows substructure. This substructure can be seen very clearly in polarized emission (Fig. 2). Two arm-like structures are visible along its southern and northern edges. The northern lobe shows a somewhat higher fractional polarization while the hotspots appear to be less polarized than the rest of the lobes. In the southern lobe, the polarization vectors follow

the edge-brightened arc-like structure (see Fig. 3), typical of such sources. The fractional polarization in the lobes is quite high although not exceptional.

PKS 2152-699 has a prominent core (see Table 1). High resolution observations made in 1988-89 with the Parkes-Tidbinbilla interferometer by Jones et al. (1994) give a core flux of 784 mJy at 2.3GHz while more recent observations obtained in 1994 with the same instrument give 583 mJy at the same frequency (Morganti et al. 1997). This may indicate some variability of the flux density of the nucleus although new observations will be necessary to confirm this. The core has an inverted spectral index,  $\alpha \sim 0.10$ .

The ratio  $R$  between the core flux density and the extended flux density derived at 4.7 GHz is  $R \sim 0.06$ . This is a typical value for broad-line galaxies as PKS 2152-699 is classified by Tadhunter et al. (1988) while it is large compared to typical FR II narrow-line radio galaxies as discussed in Morganti et al. (1997) for data collected at 2.3 GHz.

## 2.2 The nearby galaxy 2153-699

PKS 2152-699 is known to be situated in a galaxy-poor environment (Tadhunter et al. 1988). However, the presence of a nearby ( $\sim 3.8$  arcmin east) strong radio source, PKS 2153-69, was already known from the model fitting to low resolution data carried out by Ekers (1969). This source is unresolved in the maps of Christiansen et al. (1977) and Tadhunter et al. (1988) and has been identified by Jones & McAdam (1992) with a 20th magnitude galaxy with unknown redshift but likely to be in the background given its magnitude. With the new data we have mapped the region corresponding to PKS 2153-699 and resolved the source into two lobes or tails. Some trail of radio emission to the west is also observed. More faint structure may be missed because of the attenuation of the primary beam. In Fig. 4 the contours of the radio emission are shown. The cross indicates the position of the optical identification, situated between the two lobes.

## 2.3 Correlation with the optical image

A broad-band HST PC 2 image (F606W filter, single 500s exposure) of PKS 2152-699 was retrieved from the public archive. After interactively cleaning cosmic-ray events, we have used this image to produce an overlay with the new radio image at 4.7GHz. The registration between the two images was carried out by aligning the radio nucleus (RA(J2000) = 21 57 06.0, DEC(J2000) = -69 41 24.0) with the peak of the optical image ( $\sigma \sim 0.2$  arcsec). The overlay is shown in Fig. 5 while Fig. 6 presents a cartoon which shows more clearly the spatial relationship between the radio, optical emission and dust absorption components. The HST image, which includes line (predominantly [O III], H $\alpha$  and [N II]) emission and continuum, clearly shows structural details of the HIC and several additional components which fall along the same axis. The position angle between the nucleus and the observed radio component, RC, near the HIC is  $34^\circ$ . This is intermediate between that of the large-scale radio structure (PA $\sim 23^\circ$  defined from the low resolution MOST radio image, Tadhunter et al. 1988) and that from VLBI observations presented by Tingay et al. (1996). The

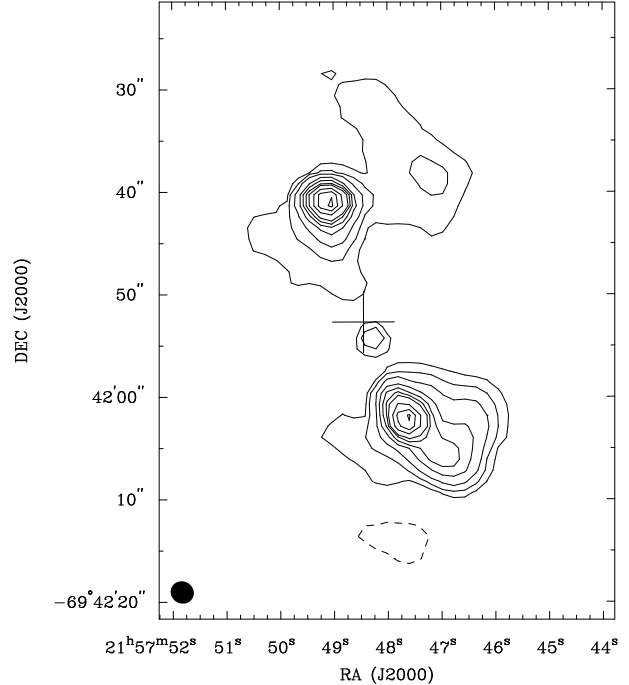


**Figure 4.** Contours of the total intensity at 4.8 GHz image of the nearby galaxy PKS 2153-699. The contour levels are -1, 1, 2, 4, 6, 8, 10, 12, 14, 16, 20, 30  $\times$  2 mJy beam $^{-1}$

VLBI observations reveal a core-jet morphology on the parsec scale and the PA of this structure is  $\sim 44^\circ \pm 5^\circ$ , close to that of the centroid of the optical HIC. The overlay shows that the HIC is situated to the east of RC which itself is coincident with a prominent part of the substructure of the cloud. This latter component was identified as a red stellar object (C) in the line-free continuum observations reported by di Serego Alighieri et al. (1988) and is therefore predominantly continuum rather than line emission with a colour very different from the rest of the HIC. The dust band crossing the galaxy in PA $\sim 110^\circ$  was inferred from the ground-based images from the colour gradient measured across the galaxy (di Serego Alighieri et al. 1988).

In addition to the emission components to the NE of the nucleus, which extend to greater distance than shown in Fig. 5 (Tadhunter et al. 1988), the HST image shows two faint regions to the SW at radial distances of approximately 11 and 16 arcsec in PA  $237^\circ$ . These were not detected in the groundbased images.

There is also a bright ‘bow’ structure, convex to the nucleus, approximately 3 arcsec along PA $\sim 57^\circ$  to the NE. This is diametrically opposite the faint SW structures. This bow was seen as a nuclear extension in the groundbased emission line imaging (see Fig. 5).

## 3 DISCUSSION

The combination of radio and optical images of PKS 2152-699 allow us to make the following statements:

- (i) There is a radio component associated with the HIC — although it is not situated at the brightest optical location. The optical emission coincident with this is red in colour and probably continuum rather than line emission.

**Figure 5** HST F606W image with radio 6cm contours superimposed. The HST image has been manually cleaned of cosmic ray events and is shown on a logarithmic scale. The radio contours are also logarithmic, ranging from 3 to 700 mJy beam<sup>-1</sup>. The radio and optical nuclei have been forced to coincide. The regions containing some of the faint features are shown with a stretched intensity scale.

(ii) There is a progression in PA from the VLBI axis (= the nucleus – HIC axis) to the nucleus – inner radio component to the large-scale radio double axis (44 – 34 – 23°).

(iii) There are a number of distinct optical structures (of which the HIC is the most prominent) lying close to the 44° PA axis. These exist on both sides of the nucleus although they are more numerous and brighter to the NE.

(iv) A dust lane crosses the nucleus in PA ~ 110° with emission along its northern edge. This could be the low ionization line emission reported by Tadhunter et al. (1988) but we cannot exclude a continuum contribution.

(v) The northern and southern lobes have a very different morphologies — the northern being diffuse with a central hotspot, the southern brighter with a ‘trailed’ hotspot.

The discovery of the bright radio component next to the HIC supports the hypothesis of a jet/cloud interaction in PKS 2152-699 and it reinforces the similarity between this object and 3C277.3, one of the best examples of jet/cloud interaction (van Breugel et al. 1985a). As pointed out by Tadhunter et al. (1988), comparison of the two objects shows a similarity in the emission-line spectra, the pres-

ence of the blue optical continuum and the offset between the cloud/nucleus axis and the radio axis. They also pointed out, however, that the cloud of ionized gas in 3C277.3 shows a large velocity gradient while the HIC in PKS 2152-699 shows broad, low intensity wings on the [O III] lines extending to the blue. The presence of extensive, chaotic dust lanes in the inner regions of the galaxy suggests that the radio jet is interacting with a fragment of a merging galaxy.

We have estimated for PKS 2152-699 the minimum pressure associated with the bright radio component to be  $\sim 3 \times 10^{-10}$  dynes cm<sup>-2</sup>. We do not have a good measure of the density of the warm line-emitting gas but if we assume  $T \approx 15000$  K (Tadhunter et al. 1988) and  $n_e \sim 200$  cm<sup>-3</sup> (a typical value for a bright extranuclear cloud) we find that, as in the case of other jet/cloud interactions, the radio and line-emitting gas pressures are quite comparable (Clark & Tadhunter 1996) suggesting that the region of high ionization has been compressed by the interaction with the radio plasma.

The presence of EELR in high and intermediate redshift radio galaxies is often associated with asymmetries in the radio morphology and polarization (Pedelty et al. 1989,

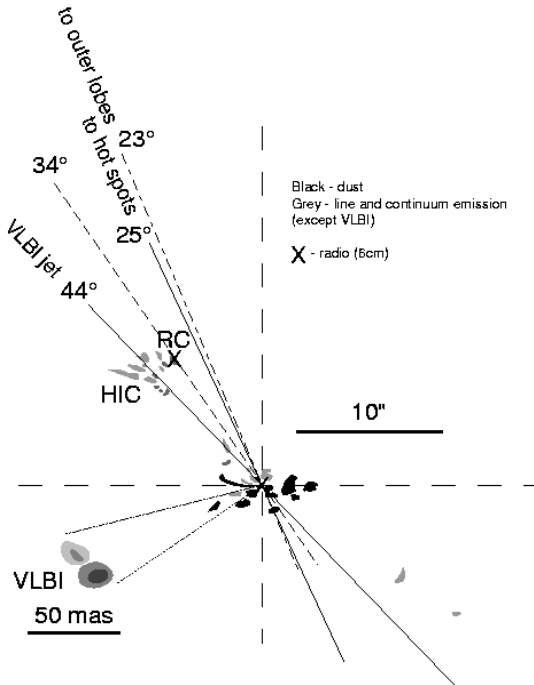


**Figure 6** Cartoon showing the different absorption and emission components in PKS2152-699. The VLBI image is represented to a different scale at the lower left.

Liu & Pooley 1991, Clark et al. 1997). In PKS 2152-699, however, there is no strong polarization asymmetry and the stronger, closer (in the sky plane) radio lobe is on the side opposite to the jet/cloud interaction. In contrast with the more powerful radio galaxies at higher redshifts, where the polarization and structural asymmetries appear to be due to large-scale ISM density variations across the source, the interaction seen here may be a transitory phenomenon without a major influence on the main radio lobe structure.

#### 4 CONCLUSIONS

We have presented new radio maps of the radio galaxy PKS 2152-699 obtained with the ATCA. These reveal a bright radio component next to the cloud of very highly ionized gas, situated about 8 kpc from the nucleus. The radio component is separated from the brightest region of the optical cloud but coincides with source of red continuum emission. This structure, together with the unusual morphology of the northern radio lobe, suggests that a jet/cloud interaction has taken place. Such interactions are relatively rare at low redshift but, when they occur, do offer the opportunity for quantitative investigation of the properties of the jets

themselves. We are currently pursuing such studies using these and other new observational data on this source.

#### ACKNOWLEDGEMENTS

This work is based on observations with the Australia Telescope Compact Array (ATCA), which is operated by the CSIRO Australia Telescope National Facility. It also uses observations made with the NASA/ESA Hubble Space Telescope obtained from the data archive at the ST-ECF. RAEF is affiliated to the Astrophysics Division, Space Science Department, European Space Agency. RM acknowledges support from the DITAC International Science & Technology Program.

#### REFERENCES

- Capetti A., Fanti R., Parma P. 1995, *A&A* 300, 643  
 Chambers K.C., Miley G.K., van Breugel W. 1987 *Nature* 329, 604  
 Christiansen W.N., Frater R.H., Watkinson A., O'Sullivan J.D., Lockhart I.A. & Goss W.M. 1977, *MNRAS* 181, 183  
 Clark N.E., Tadhunter C.N. 1996, in *Cygnus A – Study of a Radio Galaxy* eds. C.L. Carilli & D.E. Harris, CUP, p.15  
 Clark N.E., Tadhunter C.N., Morganti R., Killeen N.E.B., Hook R.N., Fosbury R.A.E., Siebert J. & Shaw M. 1997, *MNRAS*, 286, 558  
 Cox C.I., Gull S.F., Scheuer P.A.G. 1991, *MNRAS* 252, 558  
 di Serego Alighieri S., Binette L., Courvoisier T. J.-L., Fosbury R.A.E. & Tadhunter C.N. 1988, *Nature*, 334, 591  
 Ekers R.D. 1969, *AuJPS* 7,1  
 Fanaroff B.L. & Riley J.M. 1974 *MNRAS* 167, 31p  
 Fosbury R.A.E., di Serego Alighieri S., Courvoisier T.J.-L., Snijders M.A.J., Tadhunter C.N., Walsh J. & Wilson W. 1990, in *IUE Astronomy in the Era of New Space Missions* ESA SP 310, 513  
 Heckman T.M., van Breugel W.J.M. & Miley G.K. 1984, *ApJ* 286, 509  
 Jones P.A., McAdam W.B. 1992, *ApJS* 80,137  
 Jones P.A., McAdam W.B. & Reynolds J.E. 1994, *MNRAS* 268, 602  
 Linfield R. & Perley R. 1984, *ApJ* 279, 60  
 Liu R. & Pooley G., 1991, *MNRAS* 253, 669  
 McCarthy P.J., van Breugel W., Spinrad H., Djorgovski S. 1987, *ApJ* 321, L29  
 McCarthy P.J. 1993, *ARAA* 31, 639  
 Morganti R., Robinson A., Fosbury R.A.E., di Serego Alighieri S., Tadhunter C.N., Malin D.F., 1990, *MNRAS* 249,91  
 Morganti R., Oosterloo T.A., Reynolds J.E., Tadhunter C.N. & Migenes V. 1997, *MNRAS* 284, 541  
 Pedelty J.A., Rudnick L., McCarthy P.J., Spinrad H., 1989, *AJ* 97, 647  
 Reynolds J.E. 1996 in *Australia Telescope Compact Array, Users's Guide* eds. W.M. Walsh & D.J.McKay  
 Sault, R.J., Teuben, P.J., Wright, M.C.H. 1995 in *Astronomical Data Analysis Software and Systems IV*, eds. R. Shaw, H.E. Payne and J.J.E. Hayes, Astronomical Society of the Pacific Conference Series, 77, 433  
 Simkin S.M. & Ekers R.D. 1979 *ApJ* 84, 56  
 Tadhunter, C.N., Fosbury, R.A.E., Binette, L.A., Danziger, I.J., Robinson, A.: 1987, *Nature* 325, 504  
 Tadhunter C.N., Fosbury R.A.E., di Serego Alighieri S., Bland J., Danziger I.J., Goss W.M., McAdam W.B. & Snijders M.A.J. 1988, *MNRAS* 235, 403  
 Tingay S.J. et al. 1996, *AJ* 111, 718

- van Breugel W. J.M., Dey A. 1993, ApJ 414, 563  
van Breugel W., Miley G., Heckman T., Butcher H. & Bridle A. 1985a, ApJ 290, 496  
van Breugel W., Filippenko A.V., Heckman T., Miley G. 1985b, ApJ 293, 83  
van Breugel W., Heckman T.M., Miley G., Filippenko A.V. 1986, ApJ 311, 58  
Wright A.E. & Otrupcek R. 1990, Parkes Catalogue 1990, Australia Telescope National Facility

This figure "2152\_over\_pan.jpeg" is available in "jpeg" format from:

<http://arxiv.org/ps/astro-ph/9801249v1>